# Electrochemical synthesis of copper carbonates nanoparticles through experimental design and the subsequent thermal decomposition to copper oxide

To cite this article before publication: Seied Mahdi Pourmortazavi *et al* 2019 *Mater. Res. Express* in press https://doi.org/10.1088/2053-1591/aaff08

# Electrochemical synthesis of copper carbonates nanoparticles through experimental design and the subsequent thermal decomposition to copper oxide

Seied Mahdi Pourmortazavi[a], Mehdi Rahimi-Nasrabadi[b,c*], Ali Sobhani-Nasab[d], Meisam Sadeghpour Karimi[e], Mohammad Reza Ganjali[e,f], Somayeh Mirsadeghi[*g]

[a]*Faculty of Material and Manufacturing Technologies, Malek Ashtar University of Technology*
[b]*Chemical Injuries Research Center, Systems Biology and Poisonings Institute, Baqiyatallah University of Medical Sciences, Tehran, Iran*
[c] *Faculty of Pharmacy, Baqiyatallah University of Medical Sciences, Tehran, Iran*
[d]*Core Research Lab, Kashan University of Medical Sciences, Kashan, Iran*
[e]*Center of Excellence in Electrochemistry, University of Tehran, Tehran, Iran*
[f]*Biosensor Research Center, Endocrinology and Metabolism Molecular -Cellular Sciences Institute, Tehran University of Medical Sciences, Tehran, Iran*
[g] *Endocrinology and Metabolism Research Center, Endocrinology and Metabolism Clinical Sciences Institute, Tehran University of Medical Sciences, 1411713137, Tehran, Iran*

**Abstract:**

A copper anode was used in sodium carbonate solutions to prepare nanoparticles of copper carbonates. To reach the best results, the parameters affecting the preparation procedure were evaluated and optimized based on the Taguchi robust design (TRD), and it was found that the size of the resulting copper carbonates particles could be managed by applying optimal values of parameters such as electrolysis voltage, carbonate concentration, stirring rate and the temperature. To evaluate how significantly the factors influence the size of the particles, analysis of variance (ANOVA) was used, and the results indicated that the electrolysis voltage, carbonates concentration, and stirring rate affect the dimensions of the particles to a high degree. The optimal conditions were also evaluated. Further, the copper carbonate particles were used as the precursor in a solid-state thermal decomposition reaction intended for forming nanostructured CuO particles. All products were studied through SEM, XRD, TG-DTA, and FT-IR techniques and also those of optimal properties were evaluated as photocatalytic species for application in the UV-induced degradation (UVID) of methylene blue (MB).

Keywords: Copper carbonates; Copper oxide; Electrochemical synthesis; Taguchi robust design; Nanoparticles; Photocatalyst

*Corresponding authors: Tel.:+98 2182483409; Fax: +98 2182483385. E-mails: kpmrahimi@ihu.ac.ir; rahiminasrabadi@gmail.com (M. Rahimi-Nasrabadi), sshmirsadeghi@sina.tums.ac.ir (Somayeh Mirsadeghi)

## 1. Introduction

Carbonates of metallic species have been thoroughly studied recently and have found widespread industrial applications in areas such as plastic, paper, rubber and paint industries. The compounds are also considered as excellent precursors for preparing metal oxides [1]. Being a basic salt, copper carbonate has widespread applications in pigments, insecticides, fungicides, as astringent in pomades or as an antidote for phosphorus poisoning, as well as in catalysts for organic reactions, desulfurization of crudes, and wood additives [2]. Furthermore, copper oxide nanostructures have been used as pigments in ceramics, magnetic storage media, narrow-band p-type semiconductors, photothermal optical equipment, dry-cell batteries, supercapacitors, sensing instrument and photo-detectors, solar cells, catalysts and photo-catalysts, thermally-improved nano-fluids, field emission displays (FED), and extra-hydrophobic surfaces [3-6].

Removing pollutants from wastewaters and air has been an important objective during the past decades, and the increase in the populations and the subsequent incremental need for resources has added to its importance. Various organic and inorganic chemicals penetrate and pollute subterranean and surface waters, among which the most common and harmful organic species originate from pesticides, sewage and industrial wastes [7-9]. Semiconducting materials have proven to offer excellent catalytic properties in photo-induced reactions involving the degradation of organic molecules in various media and are hence classified as photocatalysts. Using these compounds various inorganic and organic pollutants can be efficiently and rapidly removed from wastewaters, through cost-effective processes with environment-friendly products, e.g. $CO_2$, $H_2O$, and inorganic ions [10-12]. In the light of those mentioned above, the copper carbonate and oxide nanostructures prepared under the optimal conditions of the present work were also evaluated as

efficient photocatalysts for eliminating MB from its water solutions, through a UV-induced degradation process.

For optimizing the process of the carbonate precursor synthesis, a fractional factorial experiment design was used. Such experiment design procedures lead to considerable decreases in the number of experiments required for the optimization, and also make it possible to acquire more information from the experimental data. The principle and procedure of the method used, i.e., Taguchi robust design (TRD) can be found in detail in different references and is hence skipped here [13-17].

## 2. Experimental Section

### *2.1. Materials*

Analytical grade $Na_2CO_3$ was obtained from Merck Company (Germany). A 1×3 $cm^2$, 99% copper sheet and a steel sheet of identical dimensions were used as the anode and cathode in the carbonate solutions, respectively. The electrodes were repeatedly polished using a wire brush and rinsed with distilled water before being immersed in the electrolyte solutions. The carbonate solutions were prepared through dissolving known amounts of $Na_2CO_3$ in distilled water. The electrodes were externally connected to a programmable power supply system for adjusting the applied voltages. The reaction cell was placed on a magnetic hot plate. The concentration, applied voltage, temperature and stirring rate applied in each experiment, were determined based on the TRD results (Table 1). The electro-synthesis reaction was performed through applying a direct current to the electrodes, and after the reaction was over, the cathode and anode were removed from the system, and the solid product was collected by centrifuging the solution. This solid was next repeatedly washed with distilled water, followed by washing with ethanol and drying at 70 ºC for

120 minutes. The values of the evaluated parameters, i.e., the carbonate concentration, applied voltage, temperature and stirring rate used according to the TRD are summarized in Table 1. The copper oxide nanoparticles were prepared through thermally decomposing the finest carbonate nanoparticles prepared in a furnace at 350 °C for 120 minutes, in an air atmosphere. The typical experiments were performed by heating 0.5 gram of the carbonate salt in an alumina crucible sealed with aluminum foil.

*2.2. Characterization of the nanoparticles*

The carbonate and oxide samples were initially studied on a ZEISS sigma/up field emission scanning electron microscope (FE-SEM). The nanoparticles were loaded onto the instrument using a gold film, prepared using a BAL-TEC, SCD005 sputter coater. X-ray diffraction (XRD) evaluations of the nanoparticles were performed using a Rigaku D/max 2500 V diffractometer with a graphite monochromator and Cu target. FT-IR spectra were also recorded in the 4000–500 $cm^{-1}$ range, using KBr pellets and a Perkin-Elmer (spectrum two) instrument. To perform the thermogravimetric (TG) and differential thermal analyses (DTA) studies on the samples, 32 mg of the copper carbonate sample were investigated on a Perkin-Elmer STA 6000 analyzer while heating the samples from 25 to 750 ºC, with a heating rate of 10 ºC/min, under a nitrogen atmosphere. Quantitative UV-VIS analyses of the MB content of photo-catalytically treated samples were performed using a Perkin- Elmer Lambda 25 UV/VIS instrument.

*2.3. Photocatalytic evaluations*

The carbonate and oxide nanoparticles were used as photocatalysts for degrading methylene blue (MB) under UV light in a cylindrical Pyrex double pipe air-lift photoreactor. The UV source was a high-pressure mercury lamp (250 W, $\lambda$>280 nm) placed inside the reactor.

0.05 g of the nanoparticles were added to 500 mL of a 5 mg/L solutions of MB in water and in order to reach the adsorption equilibrium, the resulted solution was aerated in the course of 30 min thru a photo-catalytic reactor composed of quartz double pipe air lift coupled with magnetic stirring. After determining the initial concentration of MB ($C_0$) in the reaction mixture, it was subjected to UV irradiation under a constant flow of air, at 25 °C, and the changes in the MB concentrations during the course of the reaction ($C_t$) was determined through monitoring the absorbance (At) of samples taken at 10 minutes intervals at the $\lambda_{max}$ of MB using the Lambert-Beer (eq.1) [10, 11, 17-25]:

$$A = \varepsilon bC \quad \text{Eq. 1}$$

(A: absorbance of light, ε: molar absorptivity, b: the path length of light through the sample, and C: concentration of the analyte). Further, by dividing the equation at time t to itself at time 0 eq.2 was derived:

$$\frac{A}{A_0} = \frac{C}{C_0} \quad \text{Eq. 2}$$

also, the efficiency of the photocatalytic reaction was calculated using eq.3:

$$\text{Degradation efficiency (\%)} = \frac{A_0 - A_t}{A_0} \times 100 \quad \text{Eq. 3}$$

*2.4. Kinetics of the photocatalytic reaction*

The kinetics of the UV-induced degradation of MB was evaluated using the Langmuir-Hinshelwood model which is expressed as follows [10, 11, 17, 19-25]:

$$-\frac{dC}{dt} = k_{app}C \quad \text{Eq. 4}$$

(C: concentration of the organic species, $k_{app}$: reaction rate, t: degradation time, and $-\frac{dC}{dt}$: degradation rate).

## 3. Results and discussion

### *3.1. Optimization of the electro-synthesis reaction*

Gaining control over the size of particles produced through electro-synthesis processes is an intricate process requiring a thorough understanding of the effects of the individual parameters on the size of the product. This can, however, be simplified using statistical optimization methods [14]. In this case, the effective variables were considered to be the concentration of carbonate ion, the applied voltage, reactor temperature and stirring rate, which were studied at the tree levels presented in Table 1.

The FESEM images of some of the copper carbonate samples prepared under various experimental conditions according to Table 1 are illustrated in Fig. 1, revealing the particles to have different dimensions and hence confirming the dependence of the size of copper carbonate particles on the operating conditions. Table 1 also contains the average size of the copper carbonate particles prepared under the conditions of each runs, which can be used as an input for determining the effect of each level of the parameters on the average size of the particles , and the results are plotted as bar graphs in Fig. 2. Fig. 2a illustrates the effect of $CO_3^{2-}$ concentration on the dimensions of the $CuCO_3$ particles at the three levels of 0.01, 0.05 and 0.1 M. It can be seen that 0.01 M led to the production of the finest copper carbonate particles. Further, the influence of the applied voltage (i.e., 3, 5, and 8 V) on the size of the $CuCO_3$ particles is illustrated in Fig. 2b, indicating the optimal results to be obtainable at 8 V. The results of studying the effect of the temperature of the reactor at the three levels of 0, 25 and 50 ºC (Fig. 2c) revealed the parameter to have negligible. Eventually, the effect of the stirring rate at 100, 500 and 900 rpm (Fig. 2d) proved this parameter an effective one, and the best results regarding the size of the prepared particles were observed at 500 rpm.

By performing an analysis of variance (ANOVA) on the experimental data, the significance of the variables in determining the size of the particles was evaluated, and the results are shown in Table 2. At a confidence interval of 90%, the ANOVA results proved that the concentration of the carbonate ion, the applied voltage and the stirring rate to have significant roles in defining the dimensions of the product particles. It should be noted that the study did not consider the possible interactions among the variables. The conditions leading to the optimal results were hence determined to be 0.01 M for the carbonate concentration, 8 V as the applied voltage and 500 rpm as the stirring rate of the.

Based on the TRD considerations [26-29], the optimal size of the particles can be predicted using the following expression:

$$Y_{opt} = \frac{T}{N} + (C_x - \frac{T}{N}) + (V_y - \frac{T}{N}) + (R_z - \frac{T}{N})$$

(T/N: the average size of $CuCO_3$ particles obtained through the designed experiments; T and N being the summation of all results and the total number of experiments; $Y_{opt}$: The optimal size of the $CuCO_3$ particles, $C_x$: $CO_3^{-2}$ concentration, $V_y$: applied voltage, and $R_z$: stirring rate). The confidence interval (*C.I.*) for the size of the optimally-prepared nanoparticles is obtained using the following equation [30-32]:

$$CI = \pm\sqrt{\frac{F_\alpha(f_1, f_2).V_e}{n_e}}$$

(*$V_e$*: variance of error, *$F_\alpha(f_1,f_2)$*: the critical value for *F* at the level of significance $\alpha$ (90%), *$f_1$* and *$f_2$* : the degree of freedom (DOF), while *$f_1$* is the DOF for mean (always 1) and *$f_2$* is the DOF for the error term, and *$n_e$* :the number of effective replications). *$n_e$* is determined using the equation below:

$$n_e = \frac{Number\,of\ \exp eriments}{DOF\,of\ mean(always\,1) + DOF\,of\ all\ \ factors\,at\,optimum\,conditions}$$

The calculations revealed that the size of the optimal particles to be around 14 ± 8 nm. Fig. 3, contain the FESEM and TEM images of the copper carbonate particles prepared under the above-mentioned optimal conditions revealing the average size of the particles to be about 21 nm which is comparable to the calculated results (i.e., 14 ± 8 nm). These copper carbonate nanoparticles were subjected to further structural, composition, thermal and optical analyses and further used as the precursor for preparing CuO nanoparticles.

*3.2. Characterization of the $CuCO_3$ nanoparticles*

A sample FTIR spectrum of the optimal $CuCO_3$ particles is shown in Fig. 4. The peaks were assigned to the vibrations of the carbonate ion from 400 to 1600 $cm^{-1}$. The strong wide band at around 1403 $cm^{-1}$ was attributed to the asymmetric stretching vibrations of the carbonate ion. The band at 1512 $cm^{-1}$ was assigned to the υ3 mode of the $CO_3^{2-}$ ion and those at 1098, 1054, 889, 817, 761 and 723 $cm^{-1}$ correspond to the stretching modes of this anion [1, 6, 10, 33]. Also, the stretching and bending vibrations of the hydroxyl groups of the absorbed residual water can be seen at 3436 $cm^{-1}$ [34, 35].

TG/DTA, as suitable techniques for studying the thermal stability of inorganic materials [22, 36], were also performed on the carbonate and the graphs are illustrated in Fig. 5. The TG graph reveals that the carbonate sample passes two mass loss stages. The initial step (1), which was attributed to the removal of the surface-adsorbed water accounts for a 2.5 % weight loss and is observed between 30 and 200 °C. The next step (2) comes to a weight loss of around 28 % of the sample and takes place from 200 to 350 °C. This latter weightloss was attributed to the loss of $CO_2$ and CO species from the sample. This phenomenon was very evident between 200 and 300 °C and could not be observed over 350 °C, which indicated that the carbonate salt is completely decomposed to the oxide salt after this temperature. The thermal treatment of the carbonate salt

led to a total mass loss of 30.5 % in the range of 30 to 350 °C, and 350 °C was used as the optimal temperature for the formation of CuO.

*3.3. Preparation of CuO nanoparticles*

Based on the above observations, CuO nanoparticles were prepared through calcinating optimally prepared $CuCO_3$ nanoparticles at 350 °C for 120 minutes. The SEM and TEM images of the final product are shown in Fig. 6 reavling the product to be composed of spherical particles of about 30 nm in diameter.

The nanoparticles were also studied by XRD and FT-IR techniques. Fig. 7 illustrates the XRD pattern of the CuO nanoparticles. The diffraction peaks in this figure fully comply with monoclinic CuO phase according to the JCPDS 01-080-1916 data (space group Cc) with cell parameters of a: 4.6927, b: 3.4283 and c: 5.1370 Å. The pattern is in favor of the high crystallinity and purity of the CuO nanoparticles. Using the Debye–Scherrer equation (as follow) the average crystallite size of the particles were determined to be about 33 nm.

$$D = \frac{0.9\lambda}{\beta \, \mathrm{Cos}\theta}$$

(λ:0.154059 nm, β: corrected band broadening, and θ:Bragg angle [23, 37]).

A typical FT-IR spectrum of the copper oxide sample (Fig. 8) which has lost its carbonate ions at 350 °C does not reveal the bands associated with the presence of carbonate ions and instead shows bands at 537 and 601 $cm^{-1}$, due to the presence of copper oxide. The results were found to agree with those reporting the formation of copper oxide elsewhere [3].

*3.4. Photo-degradation of methylene blue (MB)*

The results obtained through monitoring the photocatalytic activities of the optimal carbonate and oxide samples (Fig. 9) revealed the photodegradation performance of the two particles. Fig. 10 shows the changes in the MB concentration in response to UV irradiation, like diagrams of $C/C_0$

and degradation efficiency vs. illumination time. It can be seen that after 70 minutes the highest degradation yields (i.e. 99 and 96 % for $CuCO_3$ and CuO) is reached.

Normally MB as the pollutant dye in the attendance of a photo-catalyst damages as the ammonium, sulfate, nitrate, and carbon dioxide through the subsequent reaction[38, 39]:

$$MB + Pr_2(WO_4)_3 \text{ or } TiO_2 \rightarrow CO_2 + H_2O + NO_3^- + NH_4^+ + SO_4^{2-}$$

A pseudo 1st order kinetic behavior can be observed for the UV-induced degradation of MB degradation in the presence of $CuCO_3$ and CuO nanoparticles (Fig. 11) and the corresponding rate constant can be obtained from the slop of the linear regression and the photocatalytic parameters are summarized in Table 3, indicating the nanoparticles as promising photocatalysts for the removal of organic pollutants.

## 4. Conclusion

An electrosynthesis approach was used and optimized for the preparing $CuCO_3$ nanoparticles. The approach was found to offer a controllable procedure for the synthesis of $CuCO_3$ nanoparticles. The optimal reaction parameters were optimized using the Taguchi robust design (TRD). The result showed that the concentration of the copper and carbonate ions have substantial effects on the particle size of the product. The optimal carbonate nanoparticles were around 21 nm in diameter, and thermal treatment of this optimal product revealed the samples to undergo two stages decomposition leading to the formation of copper oxide particles of about 30 nm in diameter. The optimized methods offered advantages of simplicity, low cost, high output, and good product purity, further to producing ultra-fine products and the potential for scale-up. Both carbonate and oxide nanoparticles were next used evaluated as photocatalysts for removing MB from aqueous solutions and led to MB removal yields of 99 and 96 % after 70 min of UV-irradiation.

Acknowledgment

We thank our colleagues from Malek Ashtar University of Technology, Tehran University of Medical Science, Tehran University, Baqiyatallah University of Medical Sciences and Islamic Azad University who provided insight and expertise that greatly assisted the research, although they may not agree with all of the interpretations/conclusions of this paper.

[1] Rahimi-Nasrabadi M, Naderi H R, Karimi M S, Ahmadi F and Pourmortazavi S M 2017 Cobalt carbonate and cobalt oxide nanoparticles synthesis, characterization and supercapacitive evaluation *Journal of Materials Science: Materials in Electronics* **28** 1877-88

[2] Pourmortazavi S M, Kohsari I and Hajimirsadeghi S S 2009 Electrosynthesis and thermal characterization of basic copper carbonate nanoparticles *Central European Journal of Chemistry* **7** 74-8

[3] Rahimi-Nasrabadi M, Pourmortazavi S M, Davoudi-Dehaghani A A, Hajimirsadeghi S S and Zahedi M M 2013 Synthesis and characterization of copper oxalate and copper oxide nanoparticles by statistically optimized controlled precipitation and calcination of precursor *CrystEngComm* **15** 4077-86

[4] Xue B, Qv C, Qian Z, Han C and Luo G 2017 Synthesis of CuO from CuCO3·Cu(OH)2 and its catalytic activity in the degradation of methylene blue *Research on Chemical Intermediates* **43** 911-26

[5] Zhu Y W, Yu T, Cheong F C, Xu X J, Lim C T, Tan V B C, Thong J T L and Sow C H 2005 Large-scale synthesis and field emission properties of vertically oriented CuO nanowire films *Nanotechnology* **16** 88

[6] Habibi M H and Karimi B 2014 Preparation of nanostructure CuO/ZnO mixed oxide by sol–gel thermal decomposition of a CuCO3 and ZnCO3: TG, DTG, XRD, FESEM and DRS investigations *Journal of Industrial and Engineering Chemistry* **20** 925-9

[7] Omidi A and Habibi-Yangjeh A 2014 Microwave-assisted method for preparation of Sb-doped ZnO nanostructures and their photocatalytic activity *Journal of the Iranian Chemical Society* **11** 457-65

[8] Azadi M and Habibi-Yangjeh A 2015 Microwave-assisted facile one-pot method for preparation of BiOI–ZnO nanocomposites as novel dye adsorbents by synergistic collaboration *Journal of the Iranian Chemical Society* **12** 909-19

[9] Hosseinpour-Mashkani S S and Sobhani-Nasab A 2017 Investigation the effect of temperature and polymeric capping agents on the size and photocatalytic properties of NdVO4 nanoparticles *Journal of Materials Science: Materials in Electronics* **28** 16459-66

[10] Rahimi-Nasrabadi M, Pourmortazavi S M, Aghazadeh M, Ganjali M R, Sadeghpour Karimi M and Novrouzi P 2017 Samarium carbonate and samarium oxide; synthesis, characterization and evaluation of the photo-catalytic behavior *Journal of Materials Science: Materials in Electronics* **28** 5574-83

[11] Rahimi-Nasrabadi M, Pourmortazavi S M, Ganjali M R, Novrouzi P, Faridbod F and Karimi M S 2017 Preparation of dysprosium carbonate and dysprosium oxide efficient photocatalyst nanoparticles through direct carbonation and precursor thermal decomposition *Journal of Materials Science: Materials in Electronics* **28** 3325-36

[12] Zhang Y C, Du Z N, Li K W, Zhang M and Dionysiou D D 2011 High-Performance Visible-Light-Driven SnS2/SnO2 Nanocomposite Photocatalyst Prepared via In situ Hydrothermal Oxidation of SnS2 Nanoparticles *ACS Applied Materials & Interfaces* **3** 1528-37

[13] Pourmortazavi S M, Taghdiri M, Makari V and Rahimi-Nasrabadi M 2015 Procedure optimization for green synthesis of silver nanoparticles by aqueous extract of Eucalyptus oleosa *Spectrochimica Acta Part A: Molecular and Biomolecular Spectroscopy* **136** 1249-54

[14] Pourmortazavi S M, Marashianpour Z, Karimi M S and Mohammad-Zadeh M 2015 Electrochemical synthesis and characterization of zinc carbonate and zinc oxide nanoparticles *Journal of Molecular Structure* **1099** 232-8

[15] Rahimi-Nasrabadi M, Pourmortazavi S M and Khalilian-Shalamzari M 2015 Facile chemical synthesis and structure characterization of copper molybdate nanoparticles *Journal of Molecular Structure* **1083** 229-35

[16] Shamsipur M, Pourmortazavi S M, Hajimirsadeghi S S and Roushani M 2013 Applying Taguchi robust design to the optimization of synthesis of barium carbonate nanorods via direct precipitation *Colloids and Surfaces A: Physicochemical and Engineering Aspects* **423** 35-41

[17] Bayat Y, Pourmortazavi S M, Iravani H and Ahadi H 2012 Statistical optimization of supercritical carbon dioxide antisolvent process for preparation of HMX nanoparticles *The Journal of Supercritical Fluids* **72** 248-54

[18] Esmaili M and Habibi-Yangjeh A 2011 Microwave-assisted preparation of CdS nanoparticles in a halide-free ionic liquid and their photocatalytic activities *Chinese Journal of Catalysis* **32** 933-8

[19] Seied Mahdi P, Mehdi R-N, Mustafa A, Mohammad Reza G, Meisam Sadeghpour K and Parviz N 2017 Synthesis of Sm 2 (WO 4 ) 3 nanocrystals via a statistically optimized route and their photocatalytic behavior *Materials Research Express* **4** 035012

[20] Rahimi-Nasrabadi M, Pourmortazavi S M, Karimi M S, Aghazadeh M, Ganjali M R and Norouzi P 2017 Erbium(III) tungstate nanoparticles; optimized synthesis and photocatalytic evaluation *Journal of Materials Science: Materials in Electronics* **28** 6399-406

[21] Pourmortazavi S M, Rahimi-Nasrabadi M, Aghazadeh M, Ganjali M R, Sadeghpour Karimi M and Norouzi P 2017 Synthesis, Characterization, and Photocatalytic Behavior of Praseodymium Carbonate and Oxide Nanoparticles Obtained by Optimized Precipitation and Thermal Decomposition *Journal of Electronic Materials* 1-13

[22] Barjasteh-Moghaddam M and Habibi-Yangjeh A 2011 Preparation of Zn1–x Mn x O nanoparticles by a simple "green" method and photocatalytic activity under visible light irradiation *International Journal of Materials Research* **102** 1397-402

[23] Rahimi-Nasrabadi M, Pourmortazavi S M, Aghazadeh M, Ganjali M R, Karimi M S and Norouzi P 2017 Fabrication, characterization and photochemical activity of ytterbium carbonate and ytterbium oxide nanoparticles *Journal of Materials Science: Materials in Electronics* 1-11

[24] Rahimi-Nasrabadi M, Pourmortazavi S M, Aghazadeh M, Ganjali M R, Karimi M S and Norouzi P 2017 Synthesis of nano-structured lanthanum tungstates photocatalysts *Journal of Materials Science: Materials in Electronics* **28** 7600-8

[25] Ghasemi S, Setayesh S R, Habibi-Yangjeh A, Hormozi-Nezhad M and Gholami M 2012 Assembly of CeO2–TiO2 nanoparticles prepared in room temperature ionic liquid on graphene nanosheets for photocatalytic degradation of pollutants *Journal of hazardous materials* **199** 170-8

[26] Bayat Y, Hajimirsadeghi S S and Pourmortazavi S M 2011 Statistical Optimization of Reaction Parameters for the Synthesis of 2,4,6,8,10,12-Hexanitro-2,4,6,8,10,12-hexaazaisowurtzitane *Organic Process Research & Development* **15** 810-6

[27] Roy R 1990 A Primer on Taguchi Method, Van Noshtrand Reinhold Int *Co. Ltd., New York*

[28] Shahidzadeh M, Shabihi P and Pourmortazavi S M 2015 Sonochemical preparation of copper (II) chromite nanocatalysts and particle size optimization via taguchi method *Journal of Inorganic and Organometallic Polymers and Materials* **25** 986-94

[29] Ross P J and Ross P J 1988 *Taguchi techniques for quality engineering: loss function, orthogonal experiments, parameter and tolerance design*: McGraw-Hill New York)

[30] Pourmortazavi S M, Rahimi-Nasrabadi M, Karimi M S and Mirsadeghi S 2018 Evaluation of photocatalytic and supercapacitor potential of nickel tungstate nanoparticles synthesized by electrochemical method *New Journal of Chemistry* **42** 19934-44

[31] Taguchi G 1987 System of experimental design; engineering methods to optimize quality and minimize costs.

[32] Pourmortazavi S M, Rahimi-Nasrabadi M, Aghazadeh M, Ganjali M R, Karimi M S and Norouzi P 2017 Synthesis, characterization and photocatalytic activity of neodymium carbonate and neodymium oxide nanoparticles *Journal of Molecular Structure* **1150** 411-8

[33] Wang T X, Xu S H and Yang F X 2012 Green synthesis of CuO nanoflakes from CuCO3·Cu(OH)2 powder and H2O2 aqueous solution *Powder Technology* **228** 128-30

[34] Ahmadi F, Rahimi-Nasrabadi M, Fosooni A and Daneshmand M 2016 Synthesis and application of CoWO4 nanoparticles for degradation of methyl orange *Journal of Materials Science: Materials in Electronics* **27** 9514-9

[35] Rahimi-Nasrabadi M, Ahmadi F and Eghbali-Arani M 2016 Novel route to synthesize nanocrystalline nickel titanate in the presence of amino acids as a capping agent *Journal of Materials Science: Materials in Electronics* **27** 11873-8

[36] Mirzajani V, Farhadi K and Pourmortazavi S M 2018 Catalytic effect of lead oxide nano-and microparticles on thermal decomposition kinetics of energetic compositions containing TEGDN/NC/DAG *Journal of Thermal Analysis and Calorimetry* **131** 937-48

[37] Emadi H, Salavati-Niasari M and Davar F 2012 Synthesis and characterization of cobalt sulfide nanocrystals in the presence of thioglycolic acid via a simple hydrothermal method *Polyhedron* **31** 438-42

[38] Parida K and Sahu N 2008 Visible light induced photocatalytic activity of rare earth titania nanocomposites *Journal of Molecular Catalysis A: Chemical* **287** 151-8

[39] Štengl V, Bakardjieva S and Murafa N 2009 Preparation and photocatalytic activity of rare earth doped TiO2 nanoparticles *Materials Chemistry and Physics* **114** 217-26

**Figure legends:**

Fig. 1. SEM images of copper carbonate nanoparticles obtained at different runs, presented in Table 1, by electrosynthesis method: a run 2, b run 4, c run 6 and d run 9

Fig. 2. Average effects of investigated variables at different levels on the diameter of the copper carbonate nanoparticles (a) Concentration of carbonate solution, (b) Voltage, (c) Temperature and (d) Stirring rate

Fig. 3. (a) SEM image (b) TEM of copper carbonate nanoparticles obtained at optimum conditions of electrosynthesis process

Fig. 4. FT-IR spectra of the copper carbonate nanoparticles obtained under optimum conditions

Fig. 5. TG/DTA curves for thermal decomposition reaction of copper carbonate prepared via electrosynthesis method under optimum conditions; sample mass 32.0 mg; heating rate 10 ºC/min; nitrogen atmosphere

Fig. 6. (a) SEM image (b) TEM image of copper oxide nanoparticles obtained from thermal decomposition reaction of precursor

Fig. 7. XRD pattern of the copper oxide prepared by thermal decomposition reaction of copper carbonate

Fig. 8. FT-IR spectra of the copper oxide nanoparticles obtained by thermal decomposition reaction of copper carbonate

Fig. 9. UV–Vis absorbance spectrum of MB at different time intervals on irradiation using 0.1 g/L, (a) copper carbonate and (b) copper oxide nanoparticles as a photocatalyst

Fig. 10. Photocatalytic degradation of MB solution under UV irradiation using, (a) copper carbonate and (b) copper oxide nanoparticles as a photocatalyst

Fig. 11. Pseudo first order kinetics of MB degradation for, (a) copper carbonate and (b) copper oxide nanoparticles

Table 1. $OA_9$ ($3^4$) experimental design and average particle size of produced copper carbonate as results via electrochemical reaction

| Experiment number | Concentration of $CO_3^{2-}$ (M) | Voltage (V) | Temperature (°C) | Stirring rate (rpm) | Average particle size (nm) |
|---|---|---|---|---|---|
| 1 | 0.01 | 3 | 0 | 100 | 38 |
| 2 | 0.01 | 5 | 25 | 500 | 35 |
| 3 | 0.01 | 8 | 50 | 900 | 59 |
| 4 | 0.05 | 3 | 25 | 900 | 170 |
| 5 | 0.05 | 5 | 50 | 100 | 112 |
| 6 | 0.05 | 8 | 0 | 500 | 95 |
| 7 | 0.1 | 3 | 50 | 500 | 64 |
| 8 | 0.1 | 5 | 0 | 900 | 105 |
| 9 | 0.1 | 8 | 25 | 100 | 45 |

Table 2. Results of ANOVA for copper carbonate nanoparticles via electrochemical synthesis rout by $OA_9$ ($3^4$) matrix while diameters of synthesized $CuCO_3$ particles (nm) are as responses

| Factor | Code | DOF | S | V | Pooled[a] DOF | S´ | F´ | P´(%) |
|---|---|---|---|---|---|---|---|---|
| Carbonate concentration (M) | $CO_3$ | 2 | 10368.7 | 5184.3 | 2 | 10326.7 | 246.8 | 65.8 |
| Voltage (V) | V | 2 | 948.7 | 474.3 | 2 | 906.7 | 22.6 | 5.8 |
| Temperature (°C) | T | 2 | 42 | 21 | - | - | - | - |
| Stirring rate (rpm) | R | 2 | 4324.7 | 2162.3 | 2 | 4282.7 | 4282.7 | 27.3 |
| Error | E | - | - | - | 2 | - | - | 1.1 |

a The critical value was at 90% confidence level; pooled error results from pooling insignificant effect

Table 3. Pseudo First Order Reaction Rate Constant and conversion efficiency of photocatalysts at 70 min

| | K ($min^{-1}$) | Conversion (%) |
|---|---|---|
| Copper carbonate | 0.0646 | 99 |
| Copper oxide | 0.0464 | 96 |

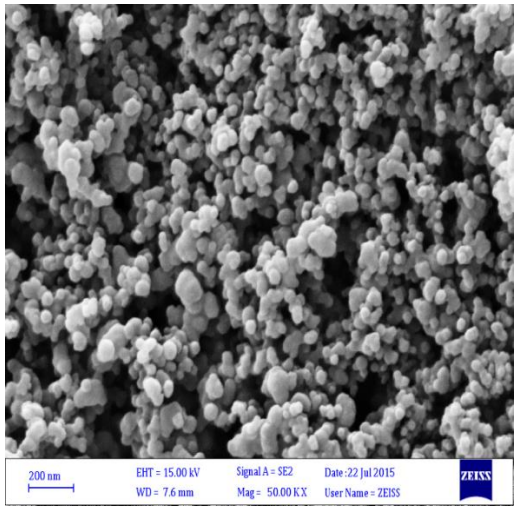


(a)

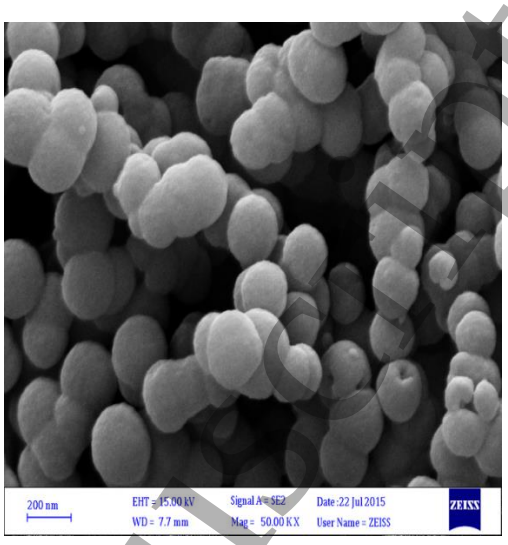


(b)

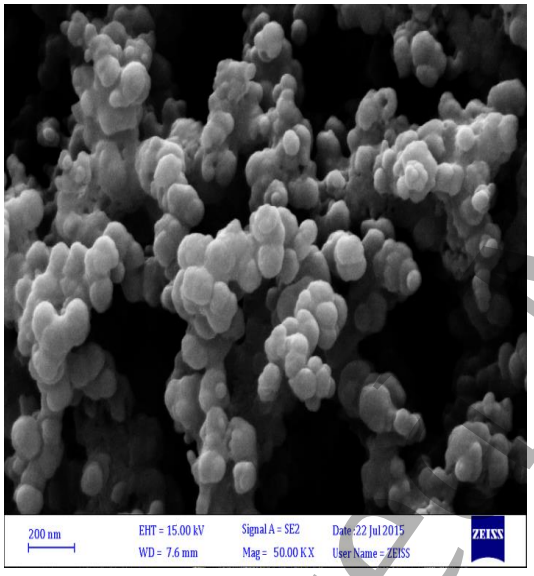


(c)

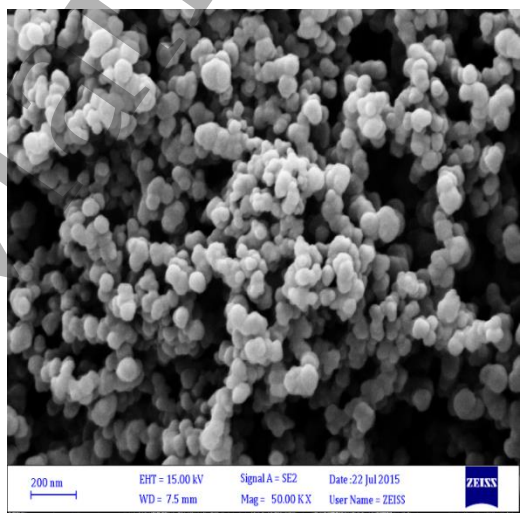


(d)

Fig. 1

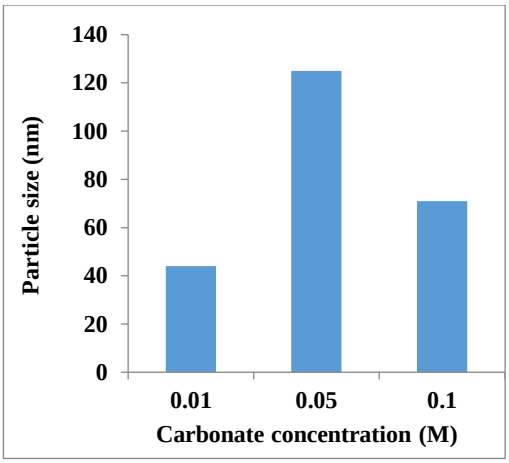


(a)

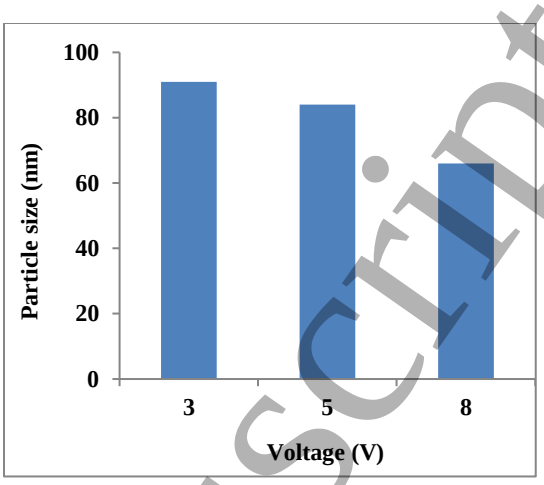


(b)

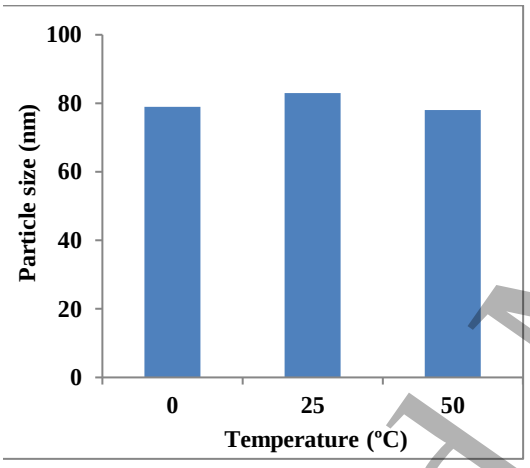


(c)

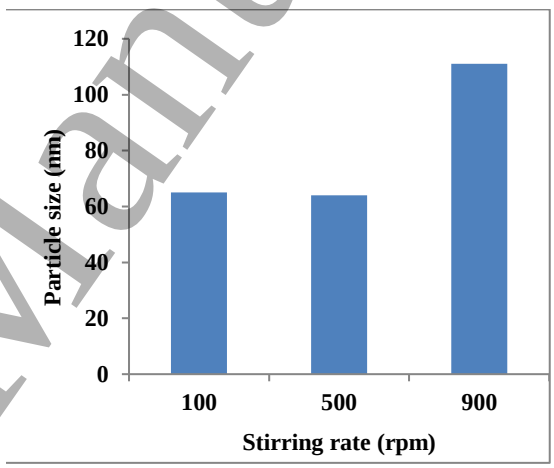


(d)

**Fig. 2**

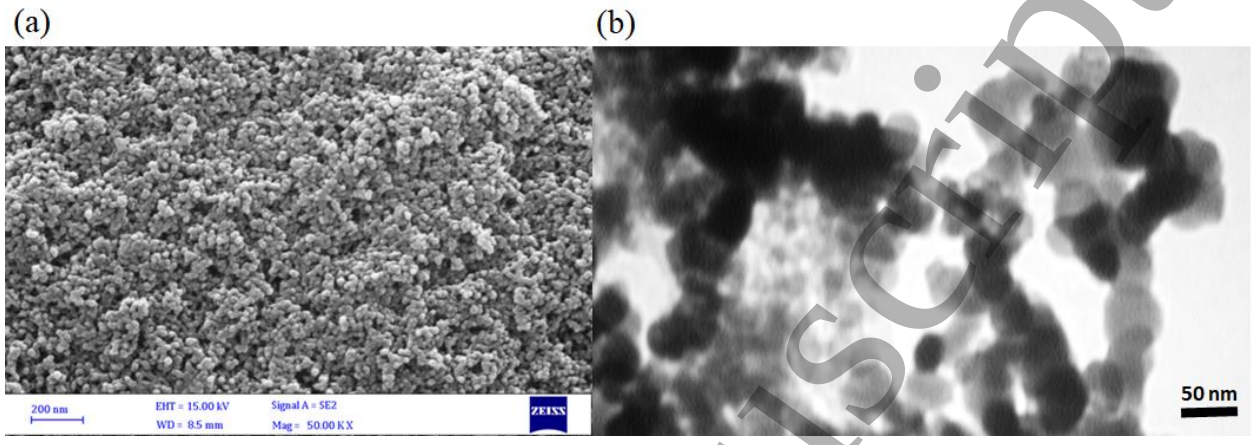


**Fig. 3**

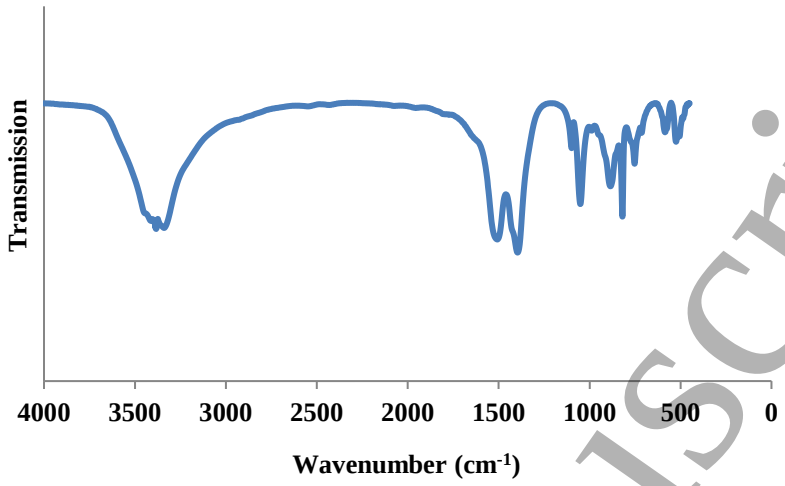


Fig. 4

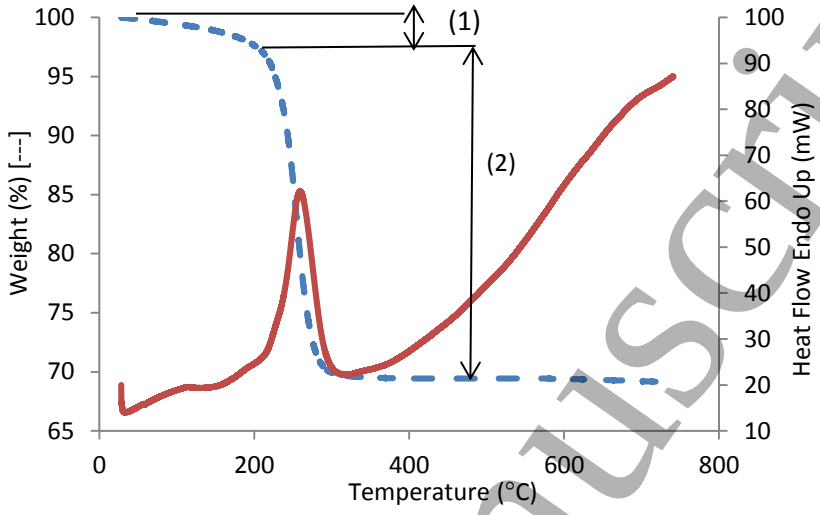


Fig. 5

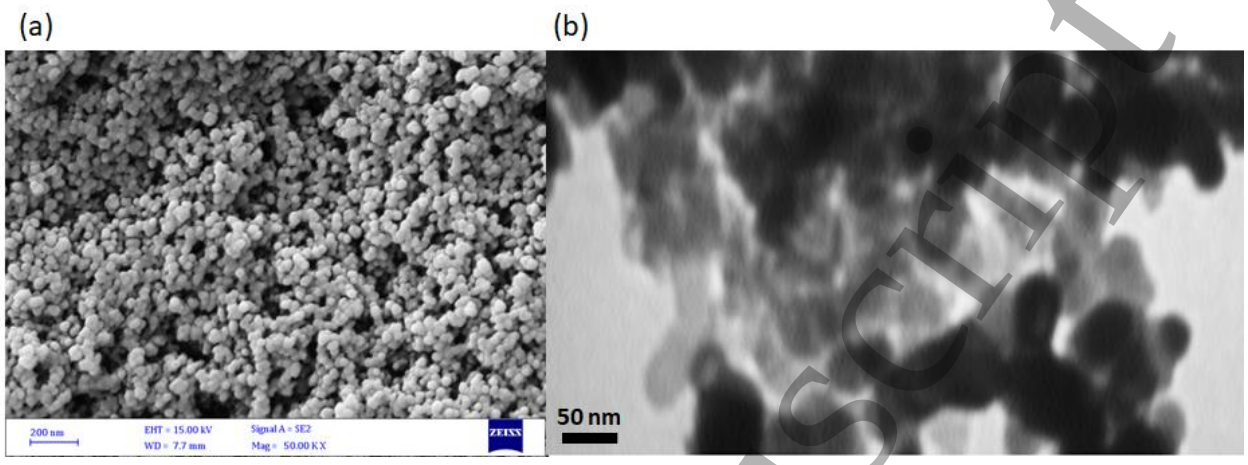


Fig. 6

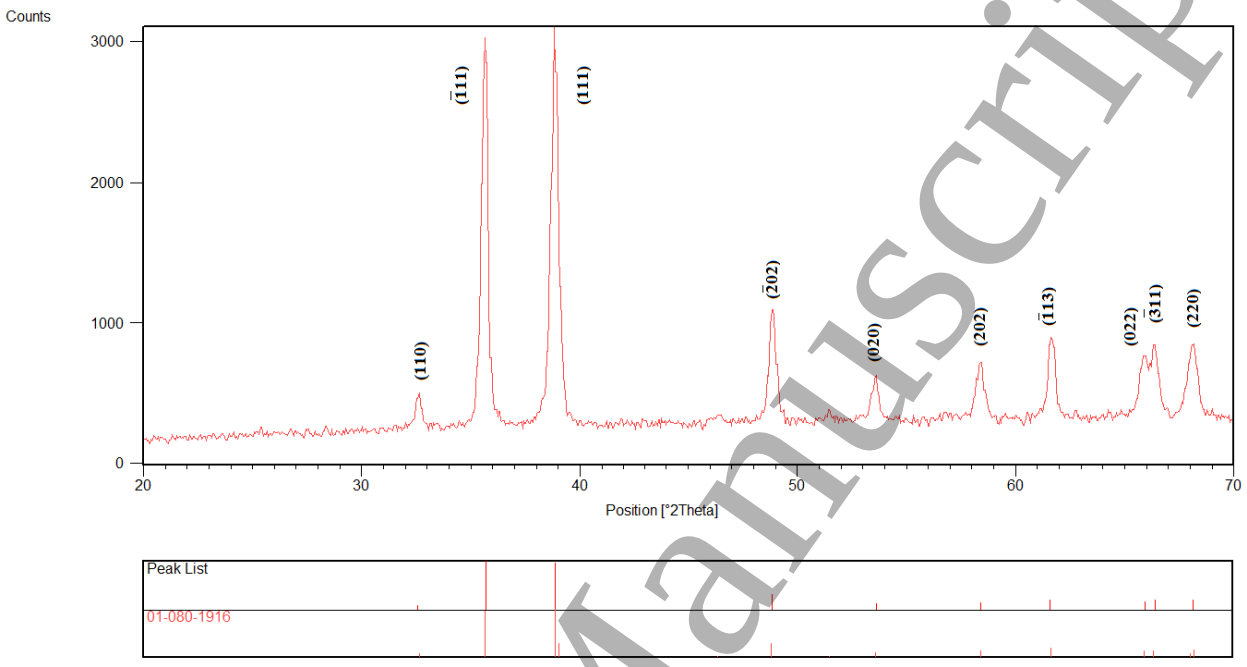


Fig. 7

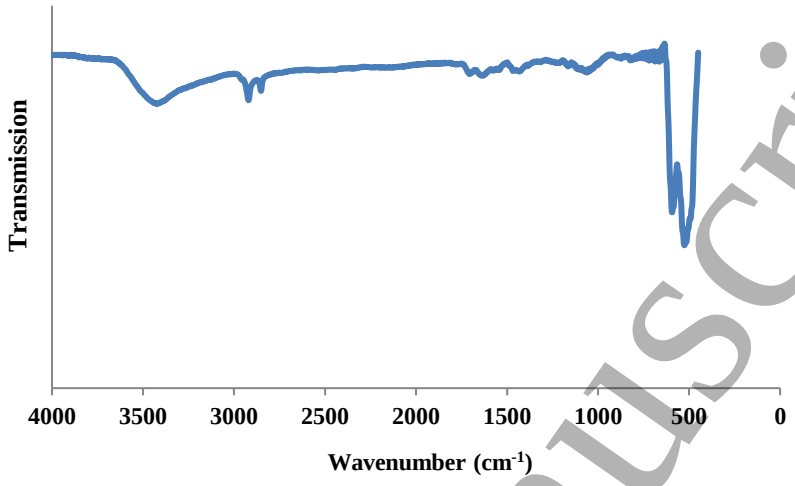


Fig. 8

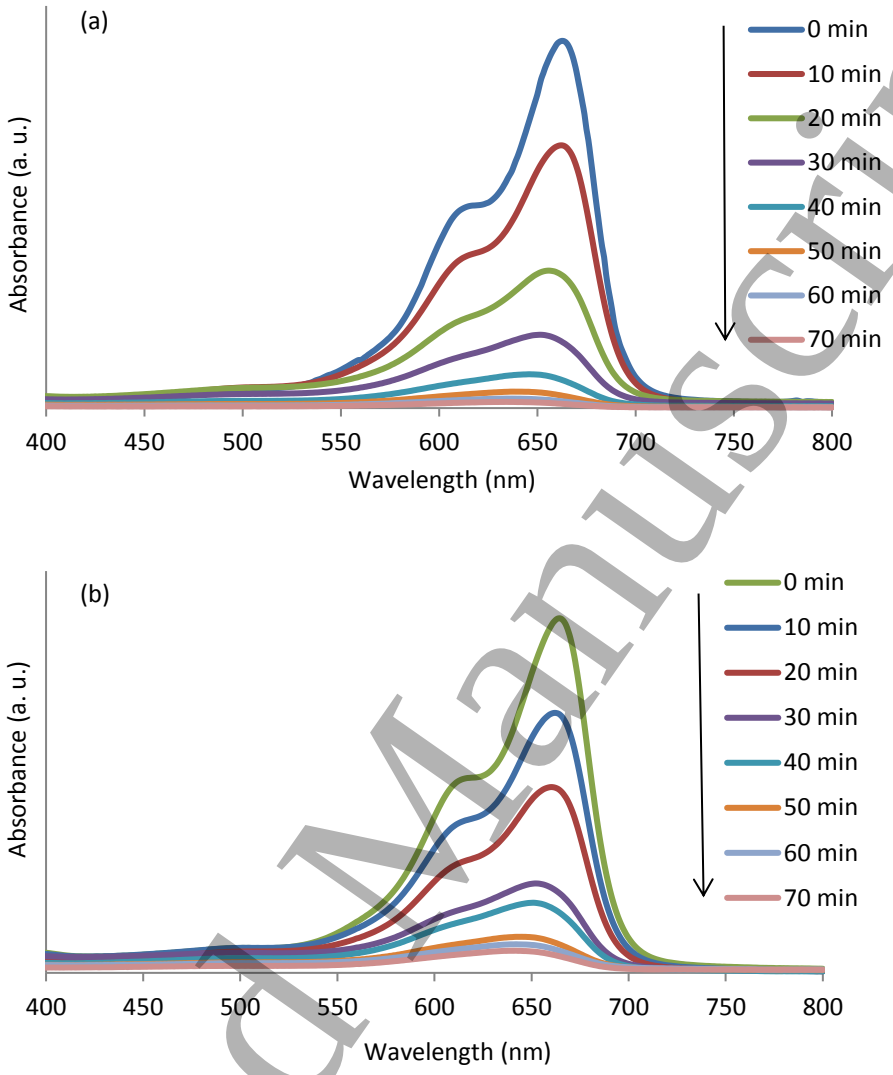


Fig. 9

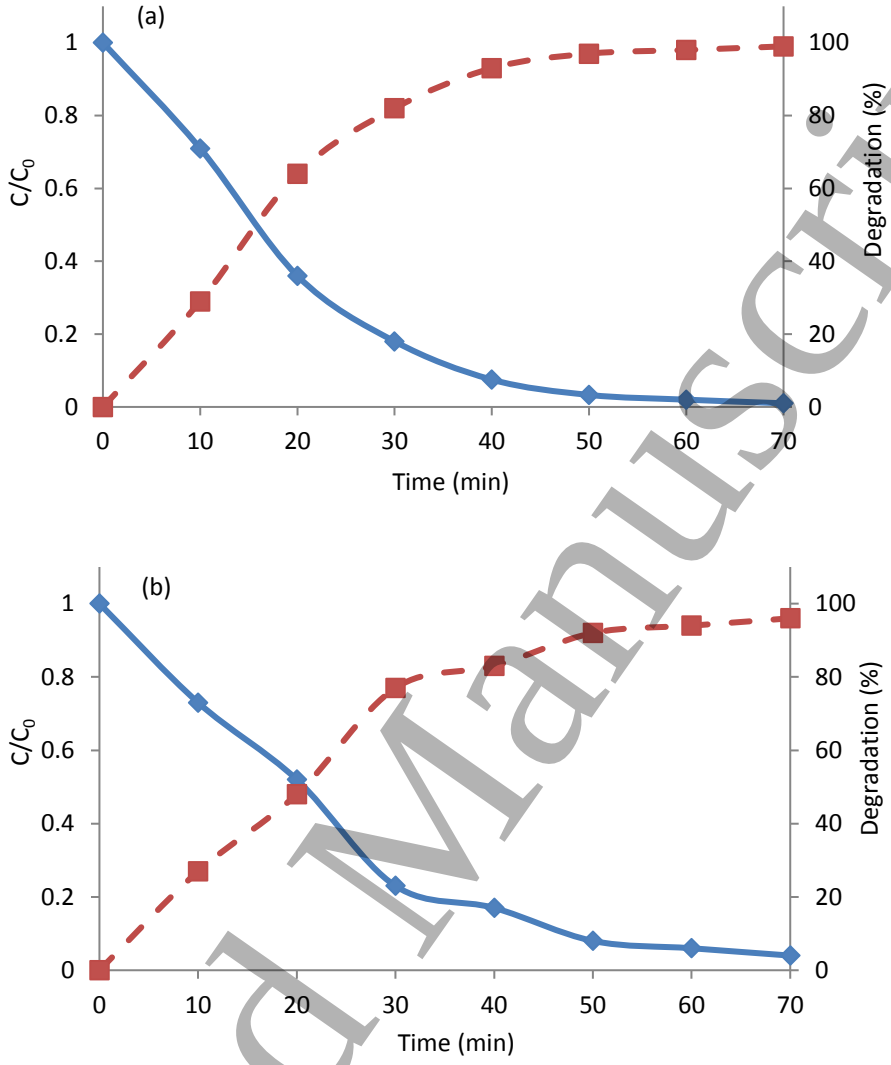


Fig. 10

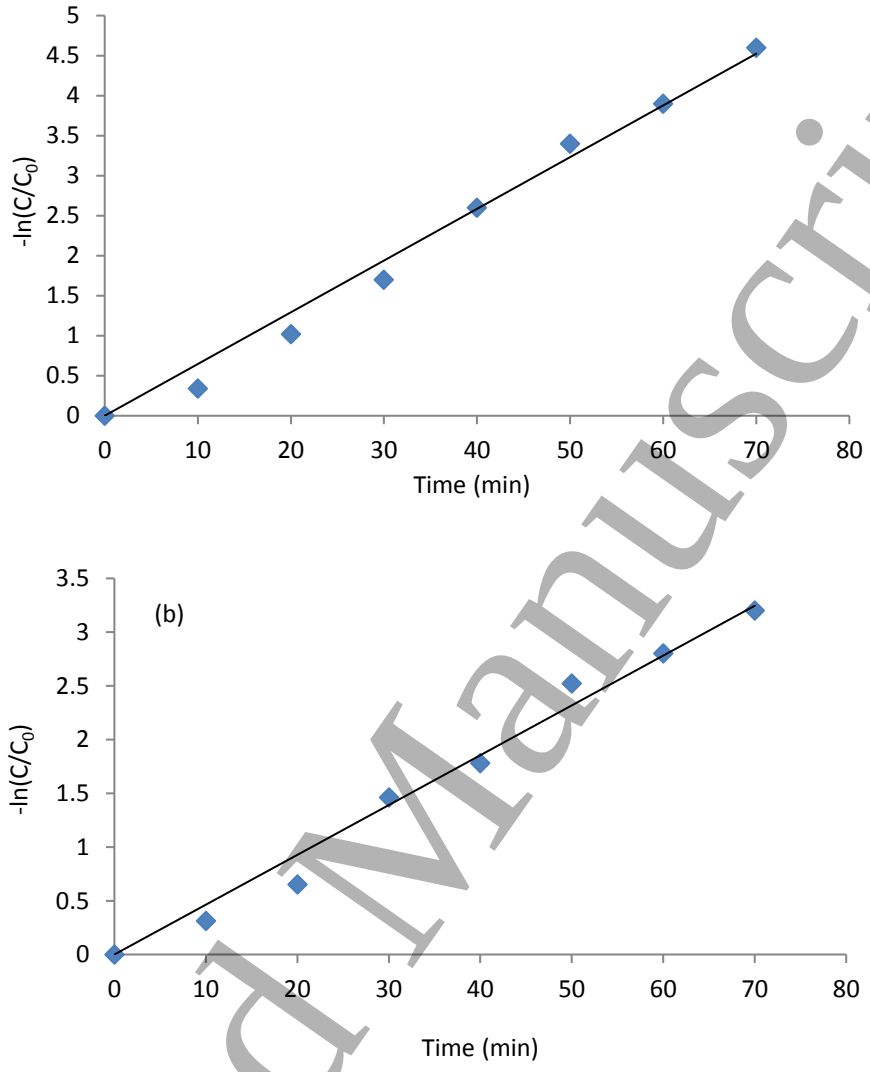


Fig. 11